



Following designations have been introduced in Fig.2:

$U_z(p)$  – set rms voltage, bit;  $\varepsilon(p)$  – comparison error, bit;  
 $u(p)$  – output (control) signal from voltage controller (PLC), bit;  
 $u_{CA}(p)$  – output signal from PCA, mA;  
 $K_{CA}(p)$  –Laplacian transfer function for PCA, bit/mA:

$$K_{CA}(p) = \frac{u_{CA}(p)}{u(p)} = \frac{u_{CA\max}}{u_{\max}}$$

$K_{CP}(p)$  – Laplacian transfer function for inverter, Hz/mA:

$$K_{PC}(p) = \frac{f(p)}{u_{CA}(p)} = \frac{f_{\max}}{u_{CA\max}}$$

$K_{MIK}(p)$  – Laplacian transfer function for MIK (machine simulating a water turbine), rad/Hz\*s:

$$(2) \quad K_{MIK}(p) = \frac{\omega(p)}{f(p)} = \frac{\frac{\omega_{\max}}{f_{\max}}}{1 + p \cdot T_{MIK}}$$

where:  $T_{MIK}$  – mechanical time constant related to inertia of induction machine simulating a water turbine and asynchronous machine operating as generator (in seconds), hence:

$$(3) \quad T_{MIK} = \frac{(J_{MIK} + J_{MAK}) \cdot \Omega_b^2}{p_b^2 \cdot S_N} = \frac{2 \cdot \pi \cdot (J_{MIK} + J_{MAK}) \cdot f_N}{3 \cdot p_b^2 \cdot U_{SkN} \cdot I_{SkN}}$$

where:  $J_{MIK}$  – moment of inertia of cage induction machine simulating a water turbine,  $\text{kgm}^2$ ;  $J_{MAK}$  – moment of inertia of asynchronous machine operating as generator,  $\text{kgm}^2$ ;  $f_N$  – rated frequency of MIK, simulating a water turbine, Hz;  $p_b$  – number of pole pairs of cage induction machine, simulating a water turbine, dimensionless quantity;  $U_{SkN}$  – rated MIK rms phase voltage, V;  $I_{SkN}$  – rated MIK rms phase current, in A;  $M_{eMIK}(p)$  – electromagnetic torque at shaft, Nm;  $P_m(p)$  – MIK power at shaft, W;  $K_{U/Pm}(p)$  – Laplacian transfer function relating rms voltage in MAP stator (machine operating as generator) to power at shaft of the same machine, V/W:

$$(4) \quad K_{U/Pm}(p) = \frac{\Delta U(p)}{\Delta P_m(p)} = \frac{\frac{\Delta U}{\Delta P_m}}{1 + p \cdot T_{U/Pm}}$$

where:  $T_{U/Pm}$  – time constant related to the process of generating rms voltage vs. MIK power at shaft (MIK – machine simulating a water turbine), s;  $U(p)$  – real value of rms voltage in MAP stator circuit (machine operating as generator), V;  $K_{pU}(p)$  – transfer function of rms voltage measurement sensor, mA/V

$$K_{pU}(p) = \frac{U'(p)}{U(p)} = \frac{U'_{\max}}{U_{\max}}$$

where:  $U'(p) = U'_{\max}$  – signal obtained at the output of measurement transducer, proportional to real value of voltage  $U(p)$ , mA;

$K_{AC}(p)$  – PAC transfer function, bit/mA:

$$K_{AC}(p) = \frac{U''(p)}{U'(p)} = \frac{U''_{\max}}{U'_{\max}}$$

and  $U''(p)$  – PAC input signal, bit.

### Selection of structure of rms voltage controller operating in MAP stator circuit

Synthesis of control system of MAP stator rms voltage, where MAP operates as generator connected to isolated grid and is driven with MIK machine supplied via frequency converter and simulating a small water turbine, has been conducted basing on “optimum magnitude” criterion suggested by C. Kessler. Starting point for the synthesis based on this criterion is transmittance (transfer function) of open-loop control system (without controller), obtained with block diagram shown in Fig.3 [1.3.5].

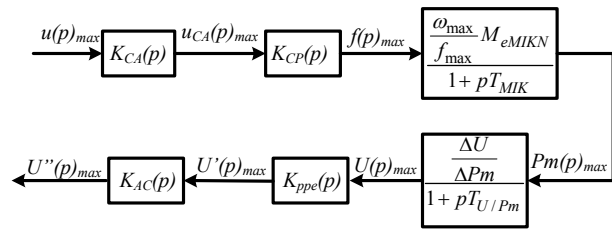


Fig. 3. Block diagram of open-loop MAP stator rms voltage control system; MAP machine operates as generator within isolated grid and is driven with MIK machine supplied via frequency converter and simulating a water turbine

Open-loop control system transfer function obtained on the basis of block diagram presented above may be defined as:

$$(5) \quad K_o(p) = \frac{K_{CA} \cdot K_{PC} \cdot \frac{\omega_{\max}}{f_{\max}} \cdot M_{eMIKN} \cdot \frac{\Delta U}{\Delta P_m} \cdot K_{pU} \cdot K_{AC}}{(1 + p \cdot T_{MIK}) \cdot (1 + p \cdot T_{U/Pm})}$$

Basing on Kessler's “Optimum magnitude” criterion, PI voltage controller was adopted. Parameters of this structure may be described by following relationships: integral time of I element:

$$(6) \quad T_Z = T_{MIK}$$

gain coefficient of P element:

$$(7) \quad K_P = \frac{T_{MIK}}{2 \cdot K_o \cdot T_{U/Pm}}$$

where:

$$(8) \quad K_o = K_{CA} \cdot K_{PC} \cdot \frac{\omega_{\max}}{f_{\max}} \cdot M_{eMIKN} \cdot \frac{\Delta U}{\Delta P_m} \cdot K_{pU} \cdot K_{AC}$$

and finally:

$$(9) \quad K_P = \frac{T_{MIK} \cdot f_{\max}}{2 \cdot T_{U/Pm} \cdot K_{CA} \cdot K_{PC} \cdot \omega_{\max} \cdot M_{eMIKN} \cdot \frac{\Delta U}{\Delta P_m} \cdot K_{pU} \cdot K_{AC}}$$

### Experimental tests of small hydro-electric power plant MEW operating within isolated grid

Schematic diagram of MEW operating within isolated grid, and simulated by MIK supplied from frequency converter, running on common shaft with slip-ring induction machine with short-circuited rotor, is shown in Fig.4. MEW turbine is simulated by voltage frequency converter  $FNI$  together with  $MIK$ . Role of cage asynchronous generator operating within isolated grid SW is played by slip-ring asynchronous machine  $MAP$ , with short-circuited rotor windings and commutation capacitors  $CI - C3$  connected to the stator windings. Control and protection processes within the small hydro-electric power plant structure are carried out in control and protection circuits with the help of software implemented in microprocessor driver  $S\mu P$ . In particular, the control and protection system in question fulfils following functions:

- Ensures automatic start-up of MEW connected to isolated grid;
- Assures stabilisation of rms voltage in isolated grid in accordance with set value;
- Ensures failure-free operation of over-speeding protection of small hydro-electric power plant (over-speeding caused by e.g. load decay of low-speed slip-ring induction machine with rotor windings short-circuited);
- Ensures failure-free operation of short-circuit protection in stator circuit of low-speed slip-ring induction machine with rotor windings short-circuited;
- Ensures failure-free operation of overvoltage protection in stator circuit of low-speed slip-ring induction machine with rotor windings short-circuited.

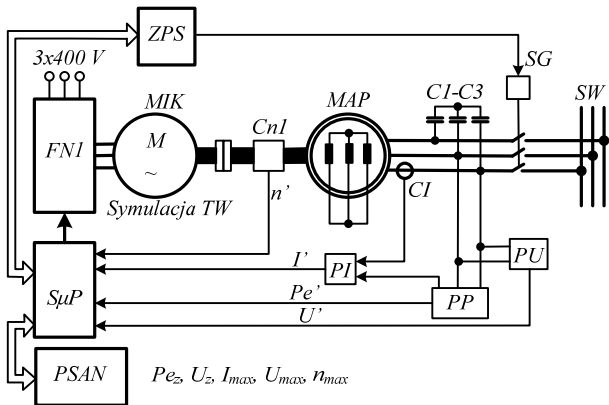


Fig.4. Laboratory model of small hydro-electric power plant, connected to isolated grid and simulated by cage induction motor supplied from frequency converter and mounted on common shaft with slip-ring induction machine having rotor windings short-circuited. The following designations are adopted here: *MIK* – cage induction machine, simulating a water turbine, *FNI* – voltage inverter; *SμP* – microprocessor driver; *Cn1* – slip-ring asynchronous machine rotational speed sensor; *MAP* – slip-ring asynchronous machine operating with short-circuited rotor windings; *CI* – current sensor (current transformer) in stator phase winding; *I* – signal proportional to real (instantaneous) current value, stator W phase; *PI* – current transducer (real value *I* to standardized value 4 ... 20 mA); *PU* – voltage transducer (real value *U* to standardized value 4 ... 20 mA); *PP* – three-phase power transducer (real value *Pe* to standardized value 4 ... 20 mA); *Pe'* – electric power transferred from slip-ring asynchronous machine stator to isolated grid circuit W; *n'* – standardized rotational speed signal 4 ... 20 mA; *I'* – standardized current signal 4 ... 20 mA; *U'* – standardized voltage signal 4 ... 20 mA; *Pe'* – standardized three-phase power signal 4 ... 20 mA; *SG* – main contactor; *SW* – isolated grid; *ZPS* – relay-contactor unit; *PSAN* – Alpha Numeric control panel; *Pe<sub>2</sub>* – set value of electrical power (option), W; *U<sub>z</sub>* – set value of rms voltage (phase-to-phase) in stator circuit (option), V; *I<sub>max</sub>* – maximum value of rms stator current value, A; *U<sub>max</sub>* – maximum value of rms phase-to-phase voltage in stator circuit, V; *n<sub>max</sub>* – maximum value of rotational speed of slip-ring asynchronous machine rpm; *CI-C3* – commutation capacitors in slip-ring asynchronous machine stator circuit.

Experimental tests have been conducted for system consisting of following elements:

- Voltage frequency converter *FNI*: type ESMD752L4TXA, rated power 7.5 kW; supply 3x400 V, rated frequency 50 Hz; rated current 14.0 A;
- Cage induction machine *MIK* simulating a water turbine: type DM1 160 M 6; rated power 7.5 kW; supply 3x400 V, rated frequency 50 Hz; rated speed 965rpm; rated power factor: 0.8; efficiency at rated load 85.2 %;
- Rotational speed sensor *Cn1* of slip-ring asynchronous machine operating with rotor windings short-circuited, range 0... 99999 rpm output signal 4 ... 20 mA; transducer fitted with display;
- Slip-ring asynchronous machine *MAP*, operating with rotor windings short-circuited: type SUDg 160 L-8; rated voltage  $U_N$  3 x 380 V; rated power  $P_N$  7.5 kW; rated speed at rated load, for motor mode  $n_N$  955 rpm efficiency  $\eta_N$ : 86.4 %; power factor 0.69 (dimensionless quantity); rated current (rms)  $I_{SN}$  19.1 A; rated electromagnetic torque at shaft  $M_{eN}$  75 Nm; moment of inertia  $J$  0.105 kgm<sup>2</sup>; number of pole pairs  $p=3$ ;
- Current transformer *CI* in stator A phase, type WSK 60; rated primary current 15 A; rated secondary current 1 A; accuracy class 0,5 %; rated power 10 VA;
- Current transducer *PI* (real value *I* to standardized value 4 ... 20 mA); input range 0 – 1 A; output range 4 ... 20 mA;

- Voltage transducer *PU* (real value *U* to standardized value 4 ... 20 mA); input range 0 – 400 V; output range 4 ... 20 mA;
  - Microprocessor driver *SμP* with following components: central processing unit CPU 226 for S7-200 driver, with ratings: memory 8 kBytes; supply voltage DC-24 V; digital inputs module EM 221 for S7-200 driver, with ratings: number of digital inputs 8; type supply voltage of digital inputs DC-24 V; I/O module, analog, EM 235 for S7-200 driver, with ratings: number of analog inputs 4; number of analog outputs 1; processing resolution 12 bit; Analog input module EM 232 for S7-200 driver, with ratings: number of analog inputs 2; resolution 12 bit; Digital outputs module EM 222 for S7-200 driver, with ratings: number of digital inputs 8; type of digital outputs supply voltage DC-24 V; type EM 222; number: 2; Alpha Numeric control panel OP15;
  - Commutation capacitors *C1- C3* 280 μF;
  - Isolated grid (SW) load: 3x100 Ω;
  - Rms voltage PI controller parameters: integral time  $T_z = T_{MIK}$ : 1.32 s; proportional gain  $K_p$ : 7.3.
- Fig. 5 shows part of the test stand (photo).

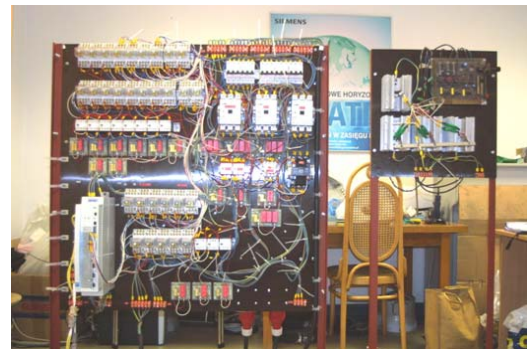


Fig.5. Control panel and frequency converter – test stand

Fig.6 presents waveforms of *MAP* output voltage (real) *U* and rotational speed *n*, generated in response to change in set voltage *U<sub>z</sub>*.

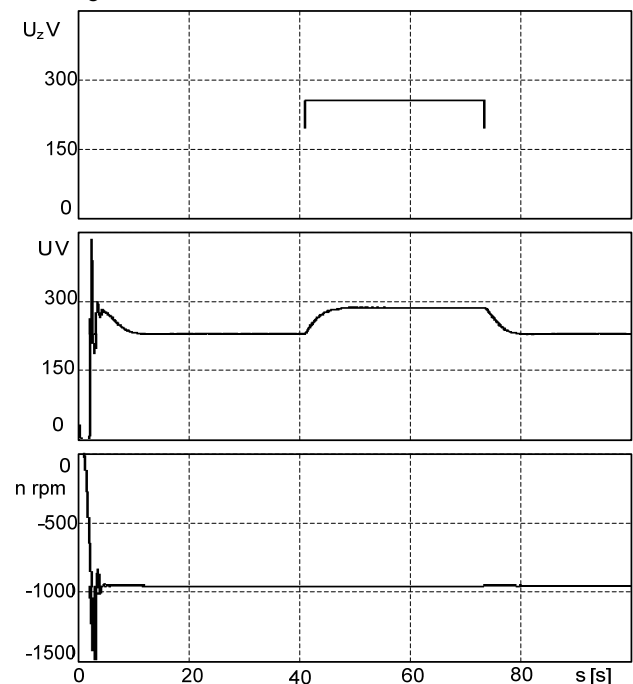


Fig. 6. Output voltage *U* and speed *n* waveforms in closed-loop control system NMAK as response to change in set voltage *U<sub>z</sub>*

## Conclusions

Synthesis of voltage control system for slip-ring asynchronous machine stator has been conducted. This machine operates with rotor windings short-circuited, is driven with cage induction motor supplied via frequency converter and simulating a water turbine, and is connected as generator to isolated grid. The control system is based on linear "optimum magnitude" criterion as formulated by C. Kessler.

Experimental tests of rms voltage control system for stator circuit of slip-ring asynchronous machine with rotor windings short-circuited, driven with cage induction motor supplied via frequency converter and simulating a water turbine, connected as generator to isolated grid have been run.

The experiments were aimed at determining the following waveforms: real rms voltage in stator circuit of slip-ring asynchronous machine with short-circuited rotor windings and real rotational speed of this machine, operating as generator connected to isolated grid. These waveforms were found for closed-loop control system as response to change in set rms voltage value.

The following conclusions have been drawn on the basis of conducted experiments:

- Selection of structure and tuning of parameters for rms voltage controller operating in stator circuit of slip-ring asynchronous machine with short-circuited rotor windings, on the basis of linear "Magnitude optimum" criterion as suggested by C. Kessler, have made it possible to attain good dynamics (with minimum overshoot) of rms voltage waveform obtained as a response to unit step change in rms voltage;
- Current and voltage frequency as well as rotational speed of slip-ring asynchronous machine operating as generator connected to isolated grid are constant versus such quantities as: shaft torque of cage induction machine simulating a water turbine, electromagnetic torque,

magnitudes of voltages and currents in slip-ring machine circuit and power output to isolated grid. However, they strongly depend on the capacitance of three-phase commutation capacitor connected into the stator and on equivalent scheme parameters of slip-ring asynchronous machine with rotor windings short-circuited. .

## REFERENCES

- [1] Orlewski W.: *Elektryczne charakterystyki generatora asynchronicznego pracującego samodzielnie w instalacji biogazowej* Proceedings of Conference: VII Ogólnopolskie Forum Odnawialnych Źródeł Energii. Międzybrodzie Żywieckie, Poland, 15 – 17 May 2002.
- [2] Kasprowicz A.: *Sterowanie samowzbudnym generatorem indukcyjnym* Przegląd Elektrotechniczny No. 11/2008, p. 334 - 339
- [3] Andreica M.; Bacha S. Roye D.; Exteberria-Otadui I.; Munteanu I.; *Micro-hydro water current turbine control for grid connected or islanding operation* Power Electronics Specialists Conference, 2008. PESC 2008. IEEE Issue Date : 15-19 June 2008 On page(s): 957 - 962
- [4] Hickiewicz J. Moch J. *Pomiarowa ocena maszyny indukcyjnej pracującej jako generator w małej elektrowni wodnej* Wiadomości Elektrotechniczne, No. 12/2005, p.14-16.
- [5] Kandyba A. Kalus M. Kurytnik I.P. *Synthesis of rms voltage current regulation circuit in the circuit of stator induction machine cage, working as a generator on the network areas of hydraulic low power engineering* Przegląd Elektrotechniczny, v.88, Nr.6, 138-141

---

**Authors:** dr inż. Andrzej Kandyba of Power Electronics, Electrical Drives and Robotics, Faculty of Electrical Engineering, Silesian University of Technology, ul. B. Krzywoustego 2 44-100 Gliwice, E-mail" [Andrzej.Kandyba@polsl.pl](mailto:Andrzej.Kandyba@polsl.pl) dr inż. Marian Kalus Institute of Innovative Technologies EMAG, Poland, 40-189 Katowice, Leopolda 31., [mkalus@emag.pl](mailto:mkalus@emag.pl) prof. dr hab. inż. Igor Piotr Kurytnik Department of Electrical Engineering and Automation University of Bielsko-Biała [ikurytnik@ath.bielsko.pl](mailto:ikurytnik@ath.bielsko.pl)